Proceedings of the 2007 IEEE Symposium on Computational Intelligence in Multicriteria Decision Making (MCDM 2007)

Multi-Criteria Identification of a Controllable Descending System

Vladimir N. Dobrokhodov[1], Roman B. Statnikov[2]

Departments of Mechanical Engineering[1] and Information Sciences[2],
Naval Postgraduate School, Monterey, CA 93943

Abstract— **This paper introduces an effective computational environment for multi-objective decision-making, optimization and identification. The paper adopts multi-objective vector identification methodology and performance assessment provided by the Parameter Space Investigation method (PSI). The main feature of this methodology is in the fact that various design objectives are taken into consideration in their natural form without reducing dimensionality of the problem and therefore without distorting its nature. Therefore, there is no need for artificial convolution and weighting of multiple criteria. Moreover, the design alternatives are assessed explicitly versus multiple given requirements. The main practical purpose of this work is of twofold. First, we introduce an optimization framework and technique that allows to determine feasible and Pareto sets of the numerous uncertainties inherent for real-world engineering systems. This framework tightly couples principal advantages of MatLab/Simulink simulation engine with the unique properties of the multi-objective PSI method. Second, we show key benefits of the MatLab/PSI bundle on the example of identification of the principal aerodynamic characteristics and apparent masses of the controllable circular parachute.**

I. Introduction

Almost every real-world problem involves concurrent optimization of multiple objectives which must be satisfied simultaneously. Multi objective optimization is a process of maximizing/minimizing a vector of incommensurable and possibly conflicting objectives. Due to the conflicting nature of the objectives, finding a single solution that optimizes all of them simultaneously is hardly possible. Therefore, in multi-objective optimization the solution is regarded as optimal in terms of Pareto optimality.

There are several problems associated with multi criteria optimization or identification. First is the problem of consistency of the adequacy criteria. We normally cannot declare a full agreement between the model and the real object primarily because only some criteria are adequate while many others are physically deficient. While the choice of the adequacy criteria might be a complicated task by itself, there are not many techniques that can provide any support in finding a physically adequate criterion. The inadequacy can also be caused by a prior uncertain nature of system parameters and their combined and unknown influences on certain physical phenomena. This is why one cannot use a single criterion to evaluate the adequacy of the model. This contributes to the principal advantage of multi-criteria identification where there is no need to introduce a single criterion artificially, which usually distorts the physics of the problem.

An overview of existing works [1-7] shows that there is only one way to resolve the deficiency problem. The solution consists in an interactive analysis of the adequacy criteria and their amendment while solving the task.

Second problem of multi criteria decision making consists in the correctness of the constraints assigned to the design variables and the functional relations. An expert often does not have sufficient information about the bounds of design variables, the bounds on functional relations might be even more difficult to assess. It is quite often that clear idea of correct constraints emerges only during the solution phase, therefore an ability to revise and adjust constraints interactively while solving the global optimization task becomes crucial.

A number of works [3-7] address the issue of multi-objective optimization or vector identification and achieve some level of success. Many works provide complete software solutions that primarily designed to solve a particular type of optimization task. Analysis of those works shows that nothing universal exists in nonlinear vector identification, primarily because of the variety of existing problems and their statements. Therefore, the lack of universal panacea still attracts numerous researchers to this task and prompts them to resolve the problem.

The Parameter Space Investigation (PSI) method [8-12] has been developed to address a correct statement and solution of the multi criteria optimization (identification) problem. The principal advantage of this method consists in the fact that the formulation and solution of the task comprise a single process. However, due to the problems discussed above the solution involves several layers of interactive work with a designer. At every step of the process, an intellectual input of the designer can be seamlessly integrated to the task therefore modifying its formulation (statement) but preserving and integrating acquired data into the final result.

The PSI method, being implemented in the software package [12] MOVI 1.3, has been implemented on top of the highly flexible MATLAB/SIMULINK system modeling and analysis environment through the shared-memory interface. This implementation easily allows one to incorporate nonlinear multi-criteria vector optimization/identification into any design task that is implemented in any of the Mathworks' products. Applying this method to an example of identifying the controllable descending system, this paper

reveals some of the advantages of simultaneous modeling and multi-criteria search, decision making and visualization.

The main practical reason for this work lies in the necessity to identify several uncertainties of the controllable circular parachute. The physical phenomenon of the controllable parachute consists in the fact that the aerodynamics depends on the canopy shape that in turn depends on the control action of the risers distorting the canopy. The major practical reason for the identification of a controllable descending system is to provide the control algorithm with an adequate model of the guided object.

A significant amount of research on circular parachute modeling has been done over the past sixty years by numerous researchers (see references in [13]). However, the existing models of a circular parachute lack unverified non-linear aerodynamics and empirical values of the apparent mass terms. Our early attempts [13] to identify these parameters improved the model, but also revealed the vital need to use a multi-criteria method.

The paper is organized as follows. It starts with a statement of the vector identification problem. The paper further discusses an implementation of a number of identification criteria that describe the proximity of the model and the real system. After formulating these criteria, the paper defines the model of controllable parachute and parameterization of the aerodynamics and apparent mass terms for which a set of design variables (DV) and their constraints are developed. Next, it introduces an idea of two-step parameter identification technique. Several features of the MOVI package are presented along the solution of the task. The paper concludes with a summary of the obtained results.

II. Statement Of The Identification Task

A. Statement of the Identification Task

The general statement [2,9] of a multi-objective identification task is as follows: optimize the vector of objective functions

$$f(x) = [f_1(x), f_2(x),..., f_k(x)]^T, \quad (1)$$

that is subject to constraints on the functional relations

$$c_j \le g(\bar{x}) \le d_j, \quad j = 1,.., m, \quad (2)$$

and design variables

$$l_i \le x_i \le \mu_i, \quad i = 1,.., n. \quad (3)$$

The term “optimize” means finding such a solution that provides the values of all the objective functions $f_k(x)$ acceptable to the designer. In other words, we wish to determine such a region from among the principal domain set of the design variables that satisfy the functional relations and yields the optimum values of all the objective functions.

Owing to the contradiction of the objective functions, finding a single solution that would optimize all the objectives simultaneously is quite difficult or even impossible. Therefore, in multi-objective optimization, the design vectors $\bar{x}_i^*$ are regarded as optimal if their components cannot be improved without deterioration to at least one of the other components. This is usually called Pareto optimality and this second mapping of the feasible to the optimal region produces the Pareto set.

B. Adequacy Criteria

The flight experiment setup (see more details in [14, 15]) included sensors and equipment that measured and stored during the flight the inertial position and velocity, the Euler angles and the control activation history. We employ this data to calculate the differences between the measurements (true data) and the corresponding modelled parameters along the flight time. Those differences are the isuue of adequcy criteria that characterize measure of closeness of the real physical system and its model.

Although the meaning of adequacy criteria is obvious (Fig.1), special consideration should be given to the correct assignment of limitations on both the unknown parameters of the system and criteria; the latter ones directly contribute to the determination of Pareto set. The determination of uknown parameters of the system is the issue of the identification process. Although their boundaries (3) are hardly initially known in the parameter space Π_1, they can be adjusted during the solution process. A correctly chosen and physically meaningful adequasy criterion shows sensitivity to the variation of identifying parameter. Such a criterion being a subject of minimization allows revealimg a feasible subset of $\Pi_2 \subset \Pi_1$ as well as its extension.

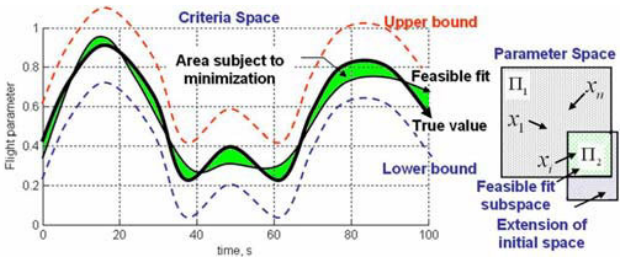

Fig. 1. Determination of adequacy criteria and Space mapping.

Figure 1 shows that the identification consists in minimizing the integral area between a true measurement and a modelled parameter corresponding to the identification variable x_i. Should the modelled parameter leave the upper and lower bounds (Fig.2), though not contributing significantly to the integral adequasy criterion, the solution becomes infeasible therefore eliminating this particular x_i. This is taken into account by using an an adequasy criteria that expels the drop-out.

Therefore, in our task besides estimating the differences of the inertial position and velocity along the flight time, we also estimate the residuals in the maximum and minimum values of the Euler angles rates.

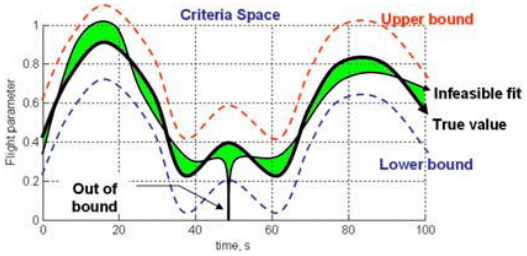

Fig. 2. System parameter is out of bounds.

We also employ the results of the spectral analysis of the Euler angles because eigen-frequencies represent the inherent oscillation dynamics of the descending system.

The final set of criteria that we employ for the identification task is presented in Table1 where we use t_{fl} to denote the flight time and the symbol " ^ " to refer to a real measurement taken in flight.

TABLE 1. IDENTIFICATION CRITERIA

	CRITERION	PHYSICAL MEANING
1,2	$\sum_0^{t_{fl}} \left\|P_H - \hat{P}_H\right\|, \sum_0^{t_{fl}} \left(P_H - \hat{P}_H\right)^2$	Sum of the residuals' modulus and their squares of the horizontal position.
3	$\sum_0^{t_{fl}} \left\|P_V - \hat{P}_V\right\|$,	Sum of the residuals' modulus of the vertical position.
4,5	$\sum_0^{t_{fl}} \left\|V_H - \hat{V}_H\right\|, \sum_0^{t_{fl}} \left\|V_V - \hat{V}_V\right\|$	Sum of the residuals' modulus of the horizontal and vertical velocity.
6,7,8	$\sum_0^{t_{fl}} \left\|\varphi - \hat{\varphi}\right\|, \sum_0^{t_{fl}} \left\|\vartheta - \hat{\vartheta}\right\|, \sum_0^{t_{fl}} \left\|\psi - \hat{\psi}\right\|$	Sum of the residuals' modulus of the Euler angles.
9	$\sum_0^{t_{fl}} \left(\psi - \hat{\psi}\right)^2$	Sum of the residuals' squares of the Yaw angle.
10, 11, 12	$\left\|\dot{\psi}_{\max} - \hat{\dot{\psi}}_{\max}\right\|, \left\|\dot{\psi}_{\min} - \hat{\dot{\psi}}_{\min}\right\|, \left\|\dot{\psi}_{avr} - \hat{\dot{\psi}}_{avr}\right\|$	Absolute differences of the max, min and average values of the Yaw rate
13, 14, 15	$\left\|f_{eig}^{\varphi} - f_{eig}^{\hat{\varphi}}\right\|, \left\|f_{eig}^{\vartheta} - f_{eig}^{\hat{\vartheta}}\right\|, \left\|f_{eig}^{\psi} - f_{eig}^{\hat{\psi}}\right\|$	The Euclid norms of the differences of the Euler angles' eigen-frequencies.

III. PSI METHOD IMPLEMENTATION

The PSI method was developed for the task of multi-objective optimization or vector identification in the form we have just presented (1-3). The method is a systematic sampling procedure of the multi-dimensional domain by using uniformly distributed sequences, which have the best uniformity characteristics in Multi-dimensional Parameter Space among those presently known. In particular, the efficiency is achieved by using of Sobol's LP_τ generator [16] that does not leave any untested spots where, theoretically, the optimal solution can be located.

Three principal steps of the PSI technique are shown in Fig.3. First, the parallelepiped-enclosed region of the design variables (DV) (3) is uniformly filled. Each point of that region is a trial point (vector) of the entire algorithm. Next, if the trial point is not feasible with respect to the functional constraints (2), it is discarded. If it is feasible, then its criterion vector (1) is computed and retained. After all the trial points have been processed, the set of all the criterion vectors forms an approximation of the feasible region $\Pi_2 \subset \Pi_1$. The last phase supposes an interaction with a designer in order to either refine the constraints on DVs (3) and the functional relations (2) or to specify the discrete approximation of a Pareto-set with respect to the applied criteria constraints (1).

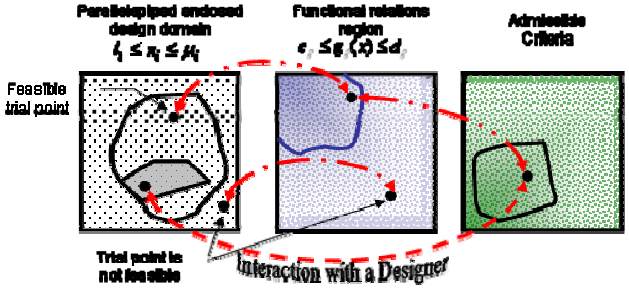

Fig.3 The principal steps of the PSI method

When we first evaluated this method, it was unable to communicate with a model created in Mathwork's MatLab/Simulink. In order to establish a communication between MOVI and MatLab/Simulink, we developed a universal interfacing library that is based on the shared-memory interface with Mathwork's computation engine. The MOVI solves any problem implemented in MatLab by iteratively calling the LP_τ generator to modify the DVs and then calling the MatLab engine to calculate the corresponding criteria. Once you specify the task in MatLab/Simulink, the MOVI does all the spade-work.

IV. MATHEMATICAL MODEL OF THE OBJECT

Analyzing the nature of parachute motion allows us to distinguish two principal ambiguities. First, the pressure distribution around a body immersed in a fluid is based on the body's shape. In turn, for a body as flexible as a parachute is, its canopy shape is determined by the pressure distribution. Therefore, the parachute not only deflects the surrounding air, but also adopts its shape, which is dictated by the airflow that the canopy generates. Beyond this, there is a combined and concurrent influence on the dynamics of motion of the aerodynamics and apparent mass terms; they contribute significantly to the dynamics of motion when a body experiences accelerations. These factors cannot be explicitly separated in order to estimate their independent influence. Furthermore, the apparent mass influence is more explicit and significant when an object undergoes acceleration due to the external forces or control actuation. Such coupling of the aerodynamics and the apparent mass terms significantly complicates one's ability to identify the controllable descending system.

Developing the six-degree of freedom (6DoF) controllable circular parachute model was previously addressed in [13]. The equations of motion for the parachute-air system (Fig.4) were based on Lagrange's approach. The final form of the equations of motion can be presented as follows:

$$\mathbf{F}^{a/d} + \mathbf{G} + \mathbf{F}_{risers} = f(\mathbf{V}, \dot{\mathbf{V}}, \boldsymbol{\Omega}, \alpha_{ij}), \quad (4)$$

$$\mathbf{M}^{a/d} + \sum_i \mathbf{M}_G^i + \mathbf{M}_{risers} = f(\mathbf{V}, \dot{\mathbf{V}}, \boldsymbol{\Omega}, \dot{\boldsymbol{\Omega}}, \alpha_{ij}), \quad (5)$$

where **F** and **M** are vectors of the external force and moment that act on the system, while $\mathbf{V} = [u, v, w]^T$ and $\boldsymbol{\Omega} = [p, q, r]^T$ are vectors of the linear and angular velocity, and α_{ij} are the apparent mass components of tensor **A.**

The specific parameters and geometry of the aerial descending system (ADS) used were those of a G-12 parachute (a 150m^2 nylon cargo parachute with 64 suspension lines) and the A-22 delivery container [15]. The top of the payload container houses guidance and control system, pneumatic muscle actuators (PMA) and instrumentation block (Fig.4).

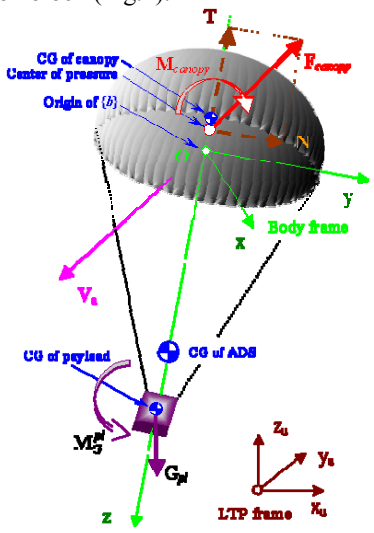

Fig 4. Modeled system

Besides the control task, the GNC system provides us with extensive telemetry data for the post-flight analysis and identification. This data includes the inertial position and velocity, and the measurements of Euler angles. A successful application of the identification technique has also been made by employing wind profiles measured during each drop. This was accomplished by using an independently launched small parachute system specifically designed for this task [15].

V. Parameterization of the Model

A. Apparent Mass Model

Similar to the rigid-body mass tensor, the apparent (virtual) mass tensor **A** has 6x6=36 unique elements. For an ideal fluid, however, **A** is a symmetrical tensor, leaving a maximum of 21 distinct terms. In the case of a body with two planes of symmetry and a coordinate frame origin located on the axis of symmetry, tensor **A** can be further reduced to the following simple form:

$$\mathbf{A} = \begin{bmatrix} \alpha_{11} & 0 & 0 & 0 & \alpha_{15} & 0 \\ 0 & \alpha_{22} & 0 & \alpha_{24} & 0 & 0 \\ 0 & 0 & \alpha_{33} & 0 & 0 & 0 \\ 0 & \alpha_{24} & 0 & \alpha_{44} & 0 & 0 \\ \alpha_{15} & 0 & 0 & 0 & \alpha_{55} & 0 \\ 0 & 0 & 0 & 0 & 0 & \alpha_{66} \end{bmatrix} \quad (6)$$

Because of the axial symmetry of the circular canopy, the following relations are valid $\alpha_{22} = \alpha_{11}$, $\alpha_{55} = \alpha_{44}$ and $\alpha_{24} = -\alpha_{15}$. That leaves only five distinct elements of the **A**.

To represent a flow around a fully deployed canopy, it is a customary to refer to the air trapped within a hemispheroid. In such a case, the air mass induces half of the spheroid and the moments of inertia correspond to those moments of the air displaced by the body

$$m_a = 0.5 m_a^s = \frac{2}{3}\pi\rho R_p^3 \varepsilon, \quad (7)$$

$$I_{xx}^{air} = \frac{1}{5} m_a R_p^2 \left(1 + \varepsilon^2\right), \quad I_{zz}^{air} = \frac{2}{5} m_a R_p^2. \quad (8)$$

In the latter equations $R_p = \frac{2}{3} R_0$ denotes the radius of the inflated parachute, where R_0 is a nominal radius of the uninflated canopy, ρ is an air density, and ε is a canopy shape ratio (for the system at hand, it equals to 0.82).

In general, the apparent mass terms depend on the canopy's configuration, porosity, acceleration and the spatial angle of attack. However, in the present study, the authors follow all other major studies [17], considered all the apparent mass terms to depend explicitly on the air density. All other possible effects were represented by variables (x_i), which are the issues of the design variables:

$$\alpha_{11} = x_1 m_a, \ \alpha_{15} = x_2 m_a z_P, \ \alpha_{33} = x_3 m_a, \ \alpha_{44} = x_4 \tilde{I}_{xxa}, \ \alpha_{66} = x_5 \tilde{I}_{zza}, \quad (9)$$

where z_P represents the distance from the origin $\{b\}$ to the canopy's center of pressure.

B. Aerodynamics

Preliminary data, provided by the CFD technique [18], requires us to introduce the influence of the spatial orientation of the system and the control inputs on the entire parachute's aerodynamics.

The aerodynamic force vector $\mathbf{F}_{canopy}$ depends on the spatial angle of attack - α_{sp}, dynamic pressure - q and control inputs. Since the control applies only to one or two possibly adjacent risers [15] and due to the parachute

symmetry, the number of control inputs n_{ctrl} can represent the degree of the control influence. Therefore, $\mathbf{F}_{canopy}$ is represented as follows:

$$\mathbf{F}_{canopy} = C_D(\alpha_{sp}, n_{ctrl}) q S_0 \frac{\mathbf{V}_a}{\|\mathbf{V}_a\|}, \quad (10)$$

where $\|\cdot\|$ denotes a Euclidian norm of the airspeed vector $\mathbf{V}_a$ and S_0 is the canopy's reference area. Analyzing the possible analytical forms of the initial CFD data, we chose the following equation for the α_{sp} in the range $[-35^\circ, 35^\circ]$:

$$C_D(\alpha_{sp}, n_{ctrl}) = x_6 + x_9 \exp(-x_7(1-\cos(\frac{\pi}{4} n_{ctrl} - \frac{\pi}{2}))^2) \times (1 - x_8 sign(\frac{\pi \alpha_{sp}}{70}) \cos(\frac{\pi}{2} + \frac{\pi \alpha_{sp}}{70})) \quad (11)$$

While developing the model, our assumptions were based on the White and Wolf's work [17]. Their work shows the uncoupled character of the longitudinal and the lateral motion of a parachute in a glide plane. The assumption implies that the roll and pitch motions of the ADS have the same moment characteristics $C_{roll} = C_m(\beta, n_{ctrl})$, $C_{pitch} = C_m(\alpha, n_{ctrl})$. Here, angle of attack α and sideslip angle β represent two plain projections of the spatial angle of attack α_{sp} on the parachutes plains of symmetry. Therefore, the vector of aerodynamic moment is represented as follows:

$$\mathbf{M}_{canopy} = 2 q S_0 R_0 [C_{roll}, C_{pitch}, C_n]^T. \quad (12)$$

Analyzing the most suitable analytical forms of the CFD data, we choose the following equation for the α, β in the range $[-35^\circ, 35^\circ]$:

$$C_m(\alpha, n_{ctrl}) = x_{11} sin(\frac{\pi}{40}\alpha - x_{12}) + x_{11} \sin x_{12} + e(-x_{10}(1 - cos(\frac{\pi}{4} n_{ctrl} - \frac{\pi}{2}))^2) - exp(-x_{10}(1 - cos(\frac{\pi}{2}))^2) \quad (13)$$

The last term C_n in the equation (12) refers to the yaw rotation that appears when the length of the riser changes during the control actuation. Typically, the yaw angle of 15…20° was accrued [15] during the transition (4…5sec) of riser state. Therefore, if the *k*-th riser undergoes transition, the following relation is valid:

$$C_n = sign(\bar{l}_{k-1} - \bar{l}_{k+1}) C_n^{\bar{l}}(\bar{l}) \bar{l}_k + C_n^r r, \quad (14)$$

where $\bar{l}_k = (l_k - l_{\min})/(l_{\max} - l_{\min})$ is a PMA's relative length, which for a shortened riser $\bar{l}_k = 0$ and for a lengthened riser $\bar{l}_k = 1$. The difference $(\bar{l}_{k-1} - \bar{l}_{k+1})$ defines the sign of the moment. The coefficient C_n^r is the damping moment coefficient.

Analyzing data from 20 flight tests [15], we found the functional dependences to be as follows: $C_n^{\bar{l}}(\bar{l}) = x_{13} \sin(\pi \cdot \bar{l})$ and the coefficient $C_n^r = x_{14}$. Result of our previous work initiates these values with $x_{13} = 0.6$ and $x_{14} = 2$.

C. Actuator Forces and Moments

The change in the aerodynamic force due to the PMA activation $\mathbf{F}_{risers}$ was modeled as a function of the PMA's relative length $\bar{l}$, number of PMA actuated (n_{ctrl}), transition time τ, and involved actuation system dynamics with unknown coefficient x_{15}:

$$\|\mathbf{F}_{risers}(t)\| = f(\bar{l}, n, \tau, x_{15}). \quad (15)$$

In turn, the actuator moment is computed as $\mathbf{M}_{risers} = \mathbf{P}_{CP} \times \mathbf{F}_{risers}$, where $\mathbf{P}_{CP} = [0, 0, z_P]^T$ is the position of the center of pressure of the canopy. For the considered system z_p= -2.0 m.

VI. Two-Step Parameter Identification Technique

Let us recall that the analysis of the flight test data reveals significant difference in the ADS dynamics during the controlled and uncontrolled drops. Therefore, the identification algorithm was first applied to the data obtained from the uncontrolled drop. The resulting values of DVs were used then to initialize the second step, in which the same technique was applied to a controlled drop. While values of DVs obtained in the first step provide estimates of ADS dynamics around zero angle of attack, their adjustment at the second step characterizes ADS dynamics at higher angles of attack with non-zero control inputs.

Another issue that should be discussed is a sufficient number of trials. Generally, it is determined based on the informal analysis of the results. Therefore, another feature we use during each step of the identification process is an application of the "double-tuning" technique. During the first step, the technique estimates the general response based on a relatively small number of trials. Then by analyzing the system's response with the predetermined level of criteria constraints, the initial DVs domains Π_1 are refined. This technique allows obtaining a sharper response from the system under consideration and consequently to obtain a superior approximation of the Pareto set.

A. Uncontrolled Drop

Since the parachute model assumes a fully deployed canopy, the analysis starts at the point on the real trajectory where the canopy was fully deployed. The initial values of the DVs' domains are shown in Table 2.

An example of the performance of double-tuning technique is presented in Fig.5 for the design variable №6. These two histograms show the distribution of feasible solutions with respect to the domain of the considered DV x6. The first result was obtained for the 128 trials and the

second one for the 2048 trials. Correspondingly, the first step produces 16% of feasible points and the second one 25%. The correction of its initial range from [0, 0.6] to [0.3, 1.0] allows obtaining a higher percentage of feasible DVs and therefore to determine the most probable range of the final solution for the uncontrolled drop phase.

TABLE 2. INITIAL DOMAINS OF THE DVS

DV	*1*	*2*	*3*	*4*	*5*	*6*	*7*
MIN	0	0.8	0.5	0.1	0	0	0.5
MAX	1.5	2	2	1	0.01	0.6	1.5
DV	*8*	*9*	*10*	*11*	*12*	*13*	*14*
MIN	0.75	0.01	0.01	0.06	0	0	1.5
MAX	1.5	0.5	0.5	0.13	0.5	0.85	5

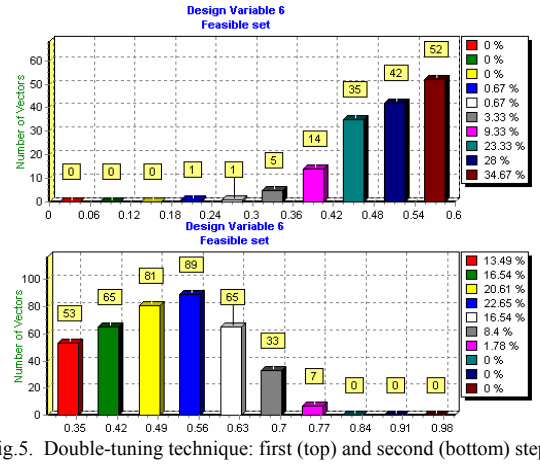

Fig.5. Double-tuning technique: first (top) and second (bottom) steps.

Another special feature of the MOVI is that this method allows distinguishing two types of criteria. The first is a "pure" criterion that is used to determine the Pareto set. The second one is a pseudo-criterion that fulfills the same functions but is not considered during the Pareto Set calculation. It allows one to "soften" the edge of the Pareto set approximation and finally produces a more stable solution.

During the identification of the ADS uncertainties, we chose only four criteria to be used in the Pareto set calculation and the rest to be pseudo-criteria. These four criteria (1,3,4,5 see Tab.1) represent the position and velocity errors while the ADS tracks the predetermined trajectory. The choice is based on the idea [15] to design the control algorithm that can steer the controllable ADS along the predetermined trajectory by compensating for the position and velocity errors through the controlled canopy distortion.

Based on the data of Test Table and applied criteria constraints, MOVI calculates the feasible solution set and the Pareto set approximation. Another useful representation of the Test Table data is a plot of one criterion versus criterion. These plots are the perfect representation of the physical nature of the model errors.

As an example, consider two plots of criteria, which in our case mean model errors. Fig.6.a represents vertical versus horizontal position errors (Criterion 1 versus Criterion 3). Fig.6.b corresponds to the vertical versus horizontal velocity errors (Criterion 4 versus Criterion 5).

In order to distinguish the obtained solutions, MOVI employs three types of points. Infeasible solutions are colored red, feasible solutions are depicted in blue, and Pareto solutions are green. Each graph shows that every criterion can be decreased, which reflects two principal factors: first, the model is sensitive to the design variables, and second, the compromise objectives of the identification process can be reached.

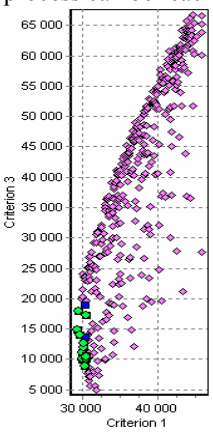

Fig. 6.a Criterion 1 versus Criterion 3

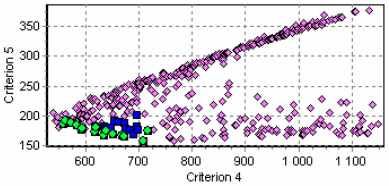

Fig. 6.b Criterion 5 versus Criterion 4

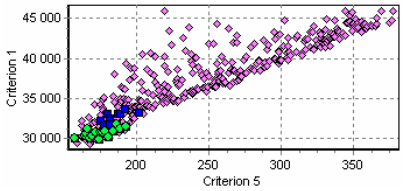

Fig. 6.c Criterion 1 versus Criterion 5

Finally, for the uncontrolled flight, we can show the model's response (Fig.7) in terms of changing the principal flight parameters, which were used to obtain the Pareto set.

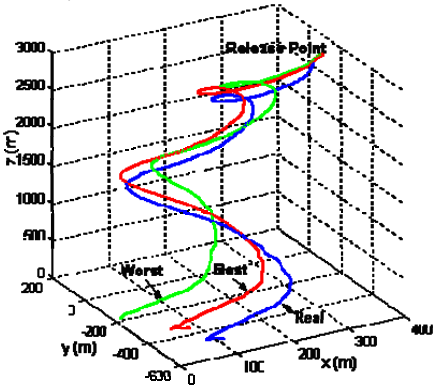

Fig. 7. Comparison of the 3D projections of the flight trajectories

Fig.7 shows 3D projections of the real flight trajectory and two solutions that correspond to the "worst" and the "best" choice of the DVs.

The main conclusion to be drawn from the uncontrolled flight identification is as follows:

- The 6DoF model is sensitive to the chosen DVs;
- The 6DoF uncontrolled dynamics are adequately close to those of the actual system;
- The PSI method allows estimating the combined influence of the chosen uncertainties at hand.

The final DVs' domains of the uncontrolled drop identification are as presented in Table3.

TABLE 3. DV DOMAINS AFTER UNCONTROLLED DROP IDENTIFICATION

DV	*1*	*2*	*3*	*4*	*5*	*6*	*7*
MIN	0	0.8	0.5	0.1	0	0.3	0.5
MAX	1.5	2	2	1	0.01	1.0	1.5
DV	*8*	*9*	*10*	*11*	*12*	*13*	*14*
MIN	0.75	0.01	0.01	0.06	0	0	1.5
MAX	1.5	0.5	0.5	0.13	0.5	0.85	5

B. Controlled Drop

The initial DV domains used to initiate the controlled drop identification were taken from the previous stage (Tab.3.). The difference that distinguishes this phase of the entire ADS identification is that DV x_{15} comes to play in the controllable motion; it is initialized with the range [0.5; 2].

C. Control Contribution

In order to estimate the required control performance and its influence on the parachute aerodynamics, we used the following approach. First, based on the Pareto set of the previous step, we chose the most reliable design vector. Next, simulating the uncontrolled flight with the wind profile measured during the controlled drop produces the trajectory "No control + Wind" (Fig.8). Subtracting this trajectory versus altitude from the flight test data (see "Real" in Fig.8), we obtain an approximation of the control contribution ("Control contribution" in Fig.8.). This particular data is used as the input data for the system identification algorithm. The idea looks reasonable because the control influence on the descent rate is insignificant [13]; hence, the new input data approximates the controlled drop in the absence of wind.

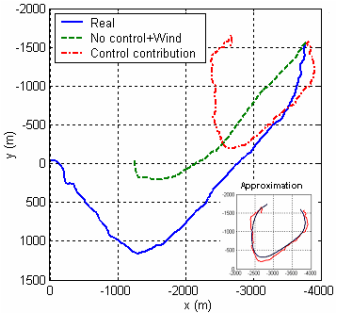

Fig. 8. Control contribution

The result of the identification procedure for this case is presented in Fig.9. Three solutions (#1-3) are shown here to reflect the model's sensitivity. They represent the position obtained by driving the 6DoF model with no wind and with control inputs recorded during the real drop.

Since the control input appears in the system through $\mathbf{F}_{risers}$ and $\mathbf{M}_{risers}$, which denote the aerodynamic force and moment caused by the change in riser length, the only variable that represents these terms is x_{15}. In turn, the moment $\mathbf{M}_{risers}$ also depends on the geometry of the entire system. However, the risers' actuation essentially changes only the shape of the canopy but not the geometry and masses location of the system.

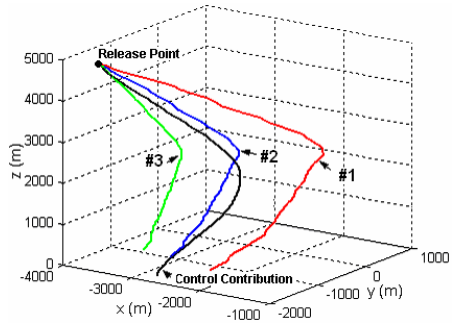

Fig. 9. Identification of the control contribution

Technically, x_{15} and its refined domain are determined by using the same procedure earlier used for the uncontrolled drop identification. However, we do not have the explicit inertial velocity profiles for this step. Therefore, in order to obtain the Pareto set we use only errors in the horizontal and vertical plain (Criteria 1 and 3). Figure 10 shows the identification result of the control contribution that includes 44 feasible solutions.

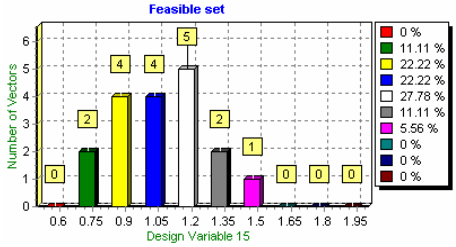

Fig.10. Histogram of the DV#15

From among them, only 18 are Pareto solutions (depicted in green on Fig.11. Obviously, the range [0.6, 1.6] represents the refined domain of the DV x_{15}.

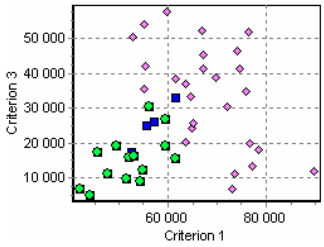

Fig.11. Plot of the Criterion 3 versus Criterion 1

D. 6.2.1 Full scale identification of the guided model

Finally, based on the results of the previous steps, which incorporates the uncontrollable flight data and the estimates of the control contribution, we move to the full-scale controllable drop identification.

Analyzing the test table provides us with the location of the optimum solution. Sequential tightening of the criteria constraints provides an approximation of the Pareto set and allows finding several solutions for further analysis.

Prior to make the final choice, three design vectors were chosen from the Pareto set in order to analyze the robustness of their criteria response (Tab.4). This step intends to check the concentration of all the design variables in the vicinity of the optimal solution and the smoothness of their criteria

responses.

TABLE 4. CORRESPONDING CRITERIA

CRITERIA	#1	#3	#4	#5
MIN:	28793	3363530	16191	786
MAX:	29097	3467024	16980	801
№110	28992	3363530	16272	794
№710	28793	3467024	16191	801
№881	29097	3439497	16980	786

Analysis of the robustness uses one more type of graph available in MOVI that is the "Criterion versus Criterion (type II)" graph; it represents the criteria response in the vicinity of a particular design vector with respect to the predetermined design variable. This technique is applied to the quasi-optimal solution №110. Figure.12 shows very smooth behavior of the criteria in the vicinity of the chosen solution.

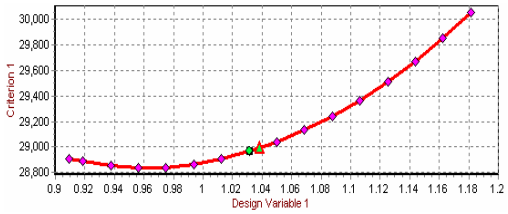

Fig.12. Section of the criterion#1 along the DV#1

Finally, Fig.13 compares the trajectories of the flight test and the controlled drop obtained in the simulation with the previously identified DV. Clearly, the results obtained in the simulation fits the flight test data fairly well. The final values of the optimization parameters are shown in Table 5; they correspond to the design vector №110.

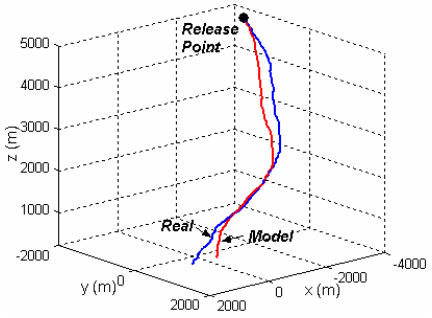

Fig. 12. The final comparison of the trajectories

TABLE 4. FINAL VALUES

DV	*1*	*2*	*3*	*4*	*5*	*6*	*7*
VALUE	1.03	0.98	1.31	0.22	0.00	0.45	1.00
DV	*8*	*9*	*10*	*11*	*12*	*13*	*14*
VALUE	1.45	0.21	0.05	0.04	0.25	0.94	3.12

VII. CONCLUSION

The paper presents an effective multi-objective decision-making methodology implemented into the Parameter Space Investigation method (PSI). Principal benefits of the technique are introduced along the process of identification of a 6DoF model of a controllable circular parachute.

Key technical contributions of the paper include:

- Integration of the MatLab/Simulink engine with MOVI1.3 software into one efficient multi-objective optimization and identification environment.
- Successful application of the nonlinear system identification technique to refine the analytical values of the aerodynamic coefficients and apparent mass terms based on the available flight test data.

The result acquitted itself well when compared with the flight test data. Nevertheless further improvement is also possible. It should include the structural optimization or reformulation of the apparent mass and control influence models. More design variables in the inertia and apparent mass tensors might be included in the model to reflect their changes during the canopy distortion. A number of different cost functions (adequacy criterion) might also be considered.

REFERENCES

[1] W. Stadler, J.P. Dauer, "Multicriteria Optimization in Engineering: a Tutorial and Survey," Progress in Aeronautics and Astronautics, AIAA, Washington, DC, 1992, vol.150, pp. 543-566.

[2] "Multicriteria Optimization in Engineering and in the Sciences," edit by W.Stadler, Plenum Press, New York and London, 1988, 405 p.

[3] M. Makowski, "Methodology and a Modular Tool for Multiple Criteria Analysis of LP Models," Proceedings of International Institute for Applied Systems Analysis, WP-94-102, December 1994.

[4] Srinivas, N., Kalyanmoy, D., "Multiobjective Otimization Using Nondominated Sorting in Generic Algorithms," Journal of Evolutionary Computation, Vol.2, N3, pp. 221-248.

[5] E. Polak, "On the Approximation of the Solution to Multiple Criteria Decision making problems," Journal of Multiple Criteria Decision Making, Kyoto 1975, pp. 271-282,

[6] W. Stadler, "Applications of Mulicriteria Optimizations in Engineering and the Sciences," MCDM: Past Decade and Future Trends, edited by Zeleny, M., JAI Press, Greenwich, CT, 1984.

[7] A. Carlos, "A Short Tutorial on Evolutionary Multiobjective Optimization," EMO 2001, LNCS 1993, pp. 21-40, 2001.

[8] R. Statnikov, J. Matusov, "Multicriteria Optimization and Engineering," Chapman and Hall, New York, 1995. 236 p.

[9] R.B. Statnikov, and J.B. Matusov, "Multicriteria Analysis in Engineering," Dordrecht/ Boston / London, Kluwer Academic Publishers, 2002.

[10] R.B. Statnikov, "Multicriteria Design. Optimization and Identification," Dordrecht/ Boston / London, Kluwer Academic Publishers, 1999.

[11] R.E. Steuer, M. Sun, "The Parameter Space Investigation Method of Multiple Objective Nonlinear programming: A computational investigation," Optimizations research, Vol. 43, Issue 4, 1995

[12] Parameter Space Investigation method. Home page of the Optimal Design Theory and Methods Laboratory: http://www.psi-movi.com .

[13] Dobrokhodov, V.N., Yakimenko O.A, and Junge, C.J., "Six-Degrees-of-Freedom Model of a Controlled Circular Parachute," AIAA Journal of Aircraft, Vol.40, №.3, 2003, pp.482-493.

[14] O. Yakimenko, V. Dobrokhodov, J. Johnson, I. Kaminer, S. Delliker, R. Benney, "On Control of Autonomous Circular Parachutes", AIAA Guidance, Navigation, and Control Conference, Monterey, CA, August 5-8, 2002.

[15] J. Johnson, O. Yakimenko, I. Kaminer, and S. Dellicker, "On the Development and Pre-Flight testing of the Affordable Guided Airdrop System for G-12 cargo parachute," Proceedings of 16th AIAA Aerodynamic Decelerator Systems Technology Conference and Seminar, Boston, MA, May 21-24, 2001.

[16] I.M. Sobol, "Uniformly Distributed Sequences With an Additional Uniform Property," USSR Comput. Math. and Math. Phys., vol. l6, 1976, pp 236-242.

[17] F.M. White, and D.F. Wolf, "A Theory of Three-Dimensional Parachute Dynamic Stability," Journal of Aircraft, Vol.5, No.1, 1968, pp.86-92.

[18] Yu.Mosseev, "Fluid-Structure Interaction Simulation of the US Army G-12 Parachute," Report 17-01-RDD Ozon, Moscow, Russia, 2001 (http://www.mtu-net.ru/mosseev/rd.htm).